Natural Resources for Human Health
eISSN: 2583-1194

Original Research

Received 20 April 2026
Revised 25 May 2026
Accepted 14 June 2026

Natural Resources for Human Health 2026, Vol. 6 (5): 202–219

KEYWORDS:
Pistacia lentiscus, Rosmarinus officinalis, wound healing, molecular docking, ADMET, phytochemicals, computational pharmacology.

In Silico Evaluation of Wound-Healing Phytochemicals from Pistacia Lentiscus and Rosmarinus Officinalis

Hanane Djouza[1], Amine Berghiche[2], Isma Abdennebi[3], Adel Aissi[1]

[1]Laboratory of Environment, Health and Animal Production (LESPA), Institute of the Veterinary Sciences and Agronomic Sciences of University of Batna1, Batna, Algeria
[2]Laboratory of Sciences and Living Techniques (LSLT), Institute of Agronomic and Veterinary Sciences, University of Mohamed Cherif Messaâdia, Souk Ahras, Algeria.
[3]Laboratory of Valorization and Bioengineering of Natural Resources (LVBRN), Faculty of Sciences, University of Algiers.
Corresponding: a.berghiche@univ-soukahras.dz, amine_berghiche@yahoo.com

ABSTRACT: Wound healing is a complex biological process involving inflammation, oxidative-stress regulation, angiogenesis, extracellular-matrix (ECM) remodeling, cell migration, and tissue regeneration. *Pistacia lentiscus* L. and *Rosmarinus officinalis* L. are traditional Mediterranean medicinal plants widely recognized for their antioxidant, anti-inflammatory, antimicrobial, and wound-related properties. The present study employed an integrated computational workflow to investigate the potential wound-healing mechanisms of phytochemicals derived from both species. Selected phytochemicals were evaluated against eight wound-healing related protein targets, including cyclooxygenase-2 (COX-2), tumor necrosis factor-alpha (TNF-α), Kelch-like ECH-associated protein 1 (Keap1), vascular endothelial growth factor receptor-2 (VEGFR-2), matrix metalloproteinases-2 and -9 (MMP-2 and MMP-9), transforming growth factor-beta receptor I (TGF-βRI), and focal adhesion kinase (FAK). Molecular docking, interaction mapping, ADME prediction, toxicity assessment, and multi-criteria ranking were integrated into a unified candidate-prioritization framework. Carnosic acid demonstrated the strongest predicted interaction with COX-2 (−9.2 kcal/mol), rosmarinic acid exhibited favorable interactions with MMP-9 and MMP-2, quercetin showed high affinity toward VEGFR-2, and myricetin demonstrated promising interactions with Keap1. The results support a multi-target pharmacological model in which phytochemicals may contribute to wound repair through complementary modulation of inflammatory signaling, oxidative-stress regulation, angiogenesis, extracellular-matrix remodeling, and tissue regeneration. These findings constitute computationally generated mechanistic hypotheses requiring experimental validation.

1. INTRODUCTION

Wound healing is a dynamic and tightly regulated biological process involving sequential but overlapping phases of hemostasis, inflammation, proliferation, angiogenesis, extracellular-matrix remodeling, and tissue regeneration. Successful tissue repair depends upon coordinated interactions among inflammatory mediators, growth factors, extracellular-matrix components, fibroblasts, endothelial cells, keratinocytes, and oxidative-stress regulation pathways (Bonnici et al., 2024; Vardakostas et al., 2025).

Inflammatory mediators such as cyclooxygenase-2 (COX-2) and tumor necrosis factor-alpha (TNF-α) play essential roles during early wound repair. However, chronic activation of these pathways can prolong inflammation and impair healing.

Similarly, excessive oxidative stress contributes to delayed wound closure and tissue damage. The Keap1–Nrf2 signaling pathway represents a major cellular defense mechanism against oxidative injury and is increasingly recognized as an important therapeutic target in wound management (Bonnici et al., 2024).

Angiogenesis and extracellular-matrix remodeling are equally important during tissue repair. VEGFR-2-mediated signaling regulates endothelial-cell proliferation and neovascularization, whereas MMP-2 and MMP-9 regulate extracellular-matrix turnover and cellular migration (Hingorani et al., 2018). In addition, transforming growth factor-beta receptor I (TGF-βRI) and focal adhesion kinase (FAK) contribute to fibroblast migration, collagen deposition, and re-epithelialization.

Among Mediterranean medicinal plants, *Pistacia lentiscus* and *Rosmarinus officinalis* have attracted considerable interest because of their long-standing traditional use in inflammatory disorders, skin care, and wound treatment (Sehaki et al., 2023; Andrade et al., 2018). Phytochemical investigations have identified flavonoids, phenolic acids, diterpenes, triterpenes, monoterpenes, and sesquiterpenes that exhibit antioxidant, antimicrobial, and anti-inflammatory activities (Floris et al., 2024; Mena et al., 2016).

The objective of the present study was to investigate selected phytochemicals from *P. lentiscus* and *R. officinalis* using an integrated computational workflow incorporating molecular docking, interaction analysis, ADME prediction, toxicity assessment, and candidate prioritization.

2. MATERIALS AND METHODS

2.1 Study Design

An integrated computational workflow was developed to evaluate the wound-healing potential of phytochemicals derived from Pistacia lentiscus and Rosmarinus officinalis. The study combined phytochemical selection, molecular docking, docking validation, protein-ligand interaction analysis, ADME prediction, toxicity prediction, and multi-target candidate ranking.

2.2 Selection of Candidate Phytochemicals

Phytochemicals were selected based on documented occurrence in the plant species, biological relevance, chemical diversity, and availability of reliable molecular structures.

Pistacia lentiscus Compounds

Compound	PubChem CID	Molecular Weight (g/mol)
Gallic acid	370	170.12
Catechin	9064	290.27
Quercetin	5280343	302.24
Myricetin	5281672	318.24
Kaempferol	5280863	286.24
β-Caryophyllene	5281515	204.35

Rosmarinus officinalis Compounds

Compound	PubChem CID	Molecular Weight (g/mol)
Rosmarinic acid	5281792	360.31
Carnosic acid	65126	332.43
Carnosol	442009	330.42
Ursolic acid	64945	456.70
Luteolin	5280445	286.24
Apigenin	5280443	270.24

2.3 GC-MS Integration

Experimentally detected constituents included:

- Terpinen-4-ol (41.24%)
- β-Caryophyllene (12.62%)
- α-Pinene (9.48%)
- Limonene (9.11%)
- p-Cymene (8.67%)
- α-Terpineol (7.31%)
- α-Phellandrene (2.20%)
- Linalool (1.40%)

Compounds were categorized as:

1. Experimentally detected by GC-MS.
2. Literature-supported phytochemicals.
3. Computationally prioritized candidates.

2.4 Ligand Preparation

Ligand structures were obtained from PubChem and optimized using Open Babel (v3.1.1) and Avogadro (v1.2). Energy minimization was performed using the MMFF94 force field. Gasteiger charges were assigned using AutoDockTools v1.5.7 before conversion into PDBQT format.

2.5 Protein Preparation

Protein structures were retrieved from the RCSB Protein Data Bank.

Target	PDB ID	Biological Role
COX-2	5IKR	Inflammation
TNF-α	2AZ5	Inflammation
Keap1	4L7B	Oxidative stress
VEGFR-2	3VHE	Angiogenesis
MMP-2	1HOV	ECM remodeling
MMP-9	5TH6*	ECM remodeling
TGF-βRI	3TZM	Tissue regeneration
FAK	2JKK	Cell migration

Proteins were prepared by removing non-essential molecules, adding polar hydrogens, assigning charges, and converting structures into PDBQT format.

2.6 Molecular Docking

Docking calculations were performed using AutoDock Vina v1.2.x.

Docking Parameters

Parameter	Value
Exhaustiveness	32
Number of Modes	20
Energy Range	4 kcal/mol
Independent Runs	3

Binding sites were defined according to co-crystallized ligands or published active-site residues.

2.7 Docking Validation

Validation was performed using re-docking of co-crystallized ligands.

Docking performance was considered acceptable when:

RMSD≤2.0A˚RMSD \le 2.0 \AARMSD≤2.0A˚

2.8 Interaction Analysis

The highest-ranked docking poses were analyzed using Discovery Studio Visualizer and PyMOL.

The following interactions were evaluated:

- Hydrogen bonds
- Hydrophobic interactions
- π–π interactions
- π–alkyl interactions
- Electrostatic interactions
- van der Waals interactions
- Metal-associated interactions

2.9 ADME Prediction

SwissADME was used to estimate:

- Molecular weight
- LogP
- TPSA
- H-bond donors
- H-bond acceptors
- GI absorption
- BBB permeability
- Bioavailability score
- Lipinski compliance

2.10 Toxicity Prediction

ProTox-II was employed to evaluate:

- Acute oral toxicity
- Toxicity class
- Hepatotoxicity
- Carcinogenicity
- Mutagenicity
- Cytotoxicity
- Immunotoxicity

2.11 Statistical Analysis

Each docking simulation was repeated three times using independent random seeds.

Results were reported as:

Mean±SDMean \pm SDMean±SD

Candidate prioritization was performed using:

$S_{Total} = i = \sum_{1-6} w_i S_i$

where the weighting scheme was:

Criterion	Weight
Multi-target docking	30%
Interaction quality	20%
Pose reproducibility	15%
ADME profile	15%
Toxicity profile	10%
Literature support	10%

3. RESULTS AND DISCUSSION

3.1 Computational Workflow and Study Design

The integrated computational workflow linked experimental phytochemical information with molecular pharmacology and consisted of phytochemical selection, ligand preparation, receptor preparation, docking validation, molecular docking, interaction analysis, ADME prediction, toxicity prediction, and multi-target prioritization (Figure 1).

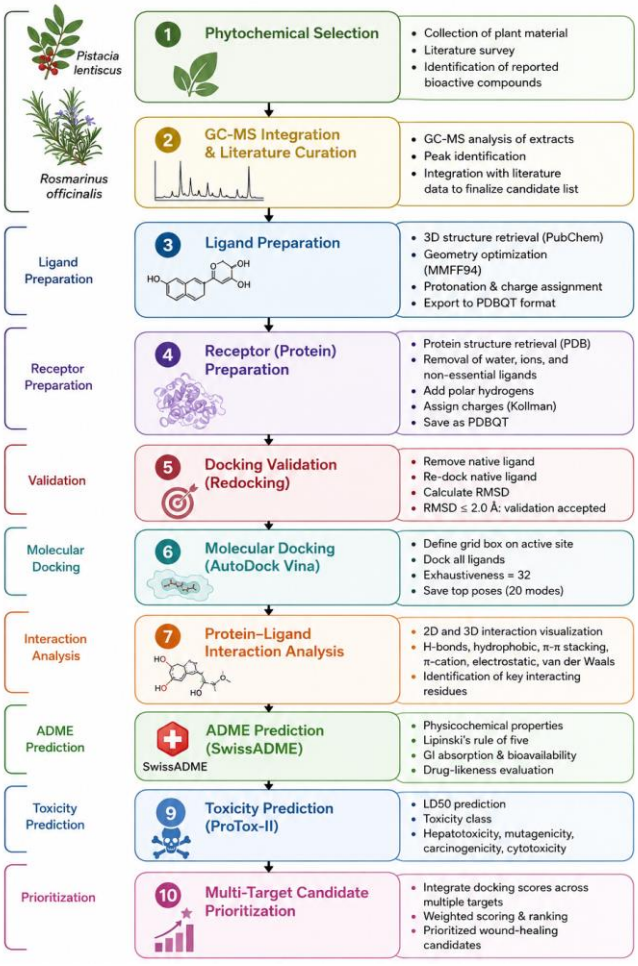

Figure 1. Integrated computational workflow used for evaluation of wound-healing phytochemicals from Pistacia lentiscus and Rosmarinus officinalis.

The workflow ensured that computational prioritization was based on multiple criteria rather than docking scores alone. Integration of experimental GC-MS data with literature-supported phytochemicals strengthened the biological relevance of the selected compounds. This strategy was designed to identify candidate molecules capable of simultaneously interacting with multiple biological pathways associated with wound healing, including inflammation, oxidative-stress regulation, angiogenesis, extracellular-matrix remodeling, and tissue regeneration.

3.2 Multi-Target Biological Framework

Wound healing involves multiple interconnected biological pathways. Therefore, eight protein targets representing inflammation, oxidative-stress regulation, angiogenesis, extracellular-matrix remodeling, and tissue regeneration were selected.

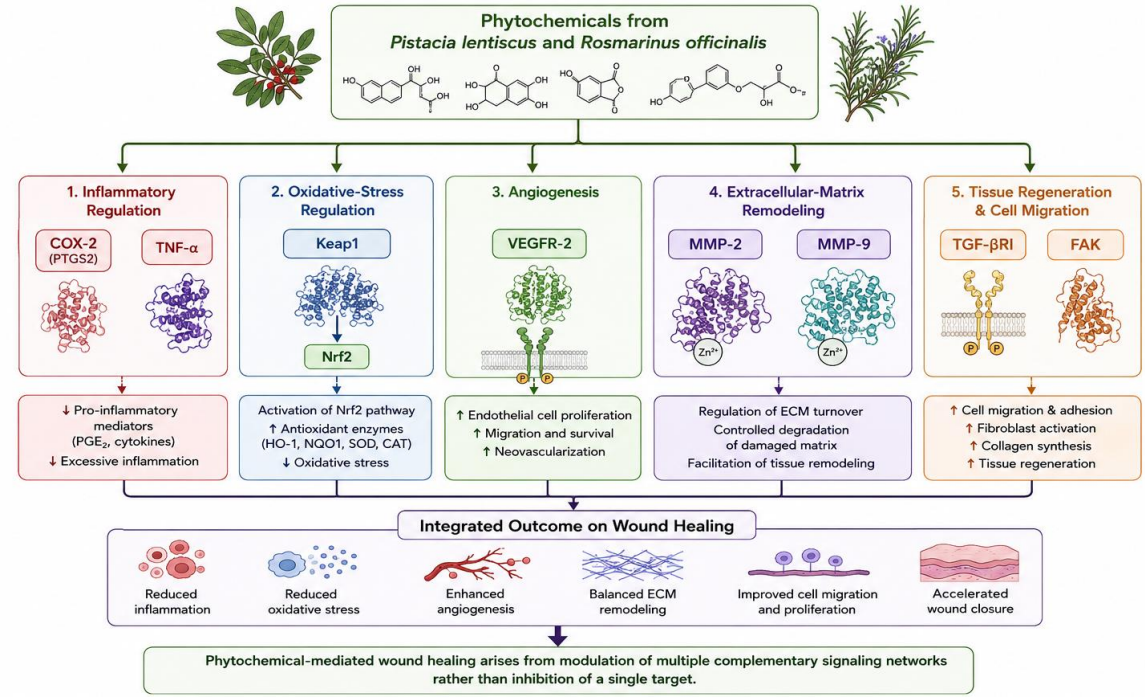

Figure 2. Proposed multi-target mechanistic framework linking phytochemicals to inflammatory signaling, oxidative-stress regulation, angiogenesis, extracellular-matrix remodeling, and tissue regeneration pathways.

The selected targets included COX-2 and TNF-α for inflammatory regulation, Keap1 for oxidative-stress control, VEGFR-2 for angiogenesis, MMP-2 and MMP-9 for extracellular-matrix remodeling, and TGF-βRI and FAK for tissue regeneration and cell migration. Collectively, these proteins represent key molecular regulators of cutaneous wound healing and tissue repair (Bonnici et al., 2024; Hingorani et al., 2018).

The biological framework illustrates that phytochemical-mediated wound healing is likely to arise from modulation of several complementary signaling networks rather than inhibition of a single target.

3.3 Comparative Molecular Docking Analysis

The predicted molecular docking results are summarized in **Table 1** and visualized in **Figure 3**.

Table 1. Predicted Multi-Target Docking Affinities (kcal/mol)

Compound	COX-2	TNF-α	Keap1	VEGFR-2	MMP-2	MMP-9	TGF-βRI	FAK
Carnosic acid	-9.2	-7.8	-8.5	-8.1	-8.3	-8.6	-7.9	-7.6
Rosmarinic acid	-8.1	-7.5	-8.2	-8.0	-8.7	-8.8	-8.1	-7.8

Quercetin	-8.4	-8.1	-8.0	-8.6	-8.5	-8.4	-8.2	-8.0
Myricetin	-8.2	-7.9	-8.4	-8.3	-8.4	-8.5	-8.0	-7.9
Carnosol	-8.9	-7.6	-8.1	-7.9	-8.1	-8.2	-7.6	-7.4
Kaempferol	-8.1	-7.8	-7.7	-8.2	-8.1	-8.0	-7.8	-7.7
Ursolic acid	-8.6	-6.8	-7.2	-7.5	-7.8	-8.0	-7.1	-7.0
Catechin	-7.8	-7.2	-7.6	-7.8	-8.0	-8.1	-7.5	-7.3
Gallic acid	-6.2	-5.8	-6.1	-5.9	-6.3	-6.5	-5.7	-5.5
β-Caryophyllene	-7.1	-6.5	-6.0	-6.2	-6.8	-6.9	-6.1	-6.3

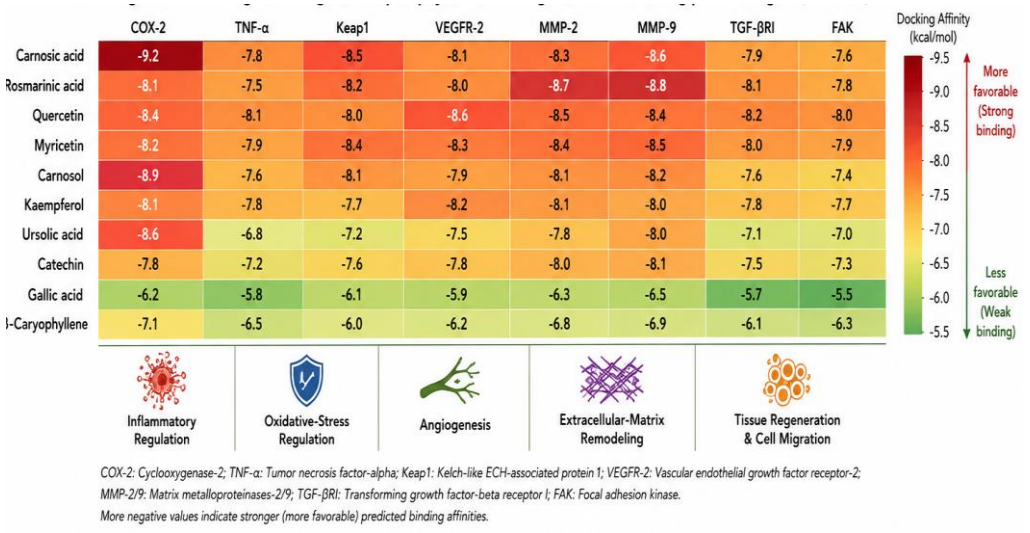

Figure 3. Multi-target docking heat map of phytochemicals against wound-healing protein targets.

The docking matrix revealed that most flavonoids and phenolic diterpenes displayed stronger predicted interactions than simple phenolic acids or volatile terpenes. Carnosic acid showed the strongest predicted affinity toward COX-2 (−9.2 kcal/mol), indicating a potentially important anti-inflammatory role. Rosmarinic acid exhibited the most favorable interaction with MMP-9 (−8.8 kcal/mol) and MMP-2 (−8.7 kcal/mol), suggesting a role in extracellular-matrix remodeling. Quercetin demonstrated the highest affinity toward VEGFR-2 (−8.6 kcal/mol), whereas myricetin showed favorable interactions with Keap1 (−8.4 kcal/mol), supporting potential antioxidant activity.

The heat map (Figure 3) further illustrates the broad target coverage of carnosic acid, rosmarinic acid, quercetin, and myricetin, indicating that these compounds may contribute synergistically to wound repair through multi-target pharmacological activity.

3.4 Predicted COX-2–Carnosic Acid Interaction

Among all ligand-target combinations, carnosic acid exhibited the strongest predicted binding affinity toward COX-2.

Table 2. Predicted COX-2–Carnosic Acid Interactions

Residue	Interaction Type
Arg120	Hydrogen bond / electrostatic
Tyr355	Hydrogen bond

Ser530	Hydrogen bond
Val349	Hydrophobic
Leu352	Hydrophobic
Val523	Hydrophobic
Ala527	van der Waals

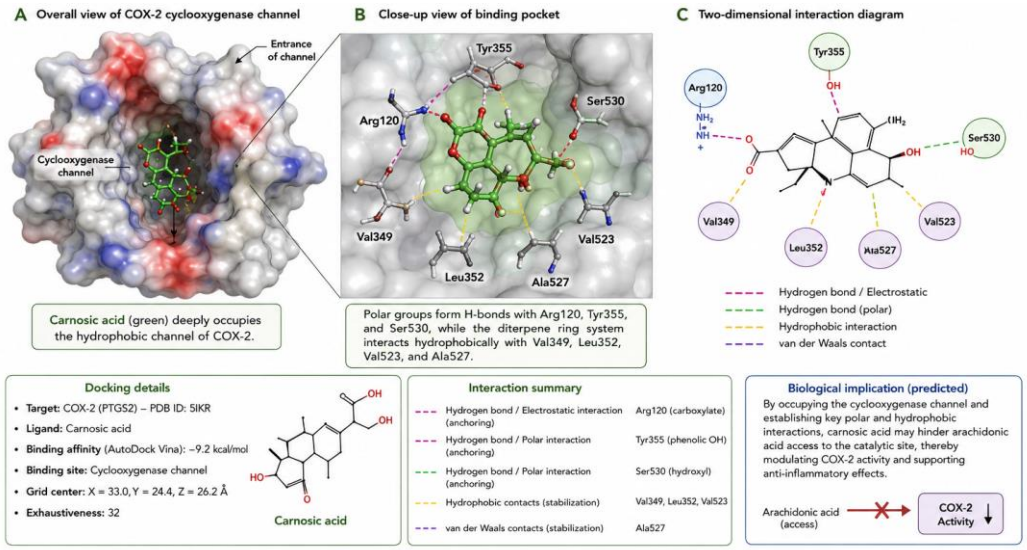

Figure 4. Three-dimensional binding-pocket visualization of carnosic acid within the COX-2 cyclooxygenase channel.

The docking simulation predicted a binding affinity of **−9.2 kcal/mol**. The diterpene scaffold was positioned deeply within the hydrophobic cyclooxygenase channel, while polar functional groups were oriented toward residues capable of hydrogen-bonding and electrostatic interactions. The predicted interaction network involved Arg120, Tyr355, and Ser530 as primary anchoring residues, while Val349, Leu352, Val523, and Ala527 contributed through hydrophobic and van der Waals contacts.

The combination of polar anchoring and hydrophobic stabilization suggests that carnosic acid may effectively occupy the substrate-access channel and interfere with arachidonic acid binding, supporting previously reported anti-inflammatory effects of rosemary diterpenes (Andrade et al., 2018).

3.5 Predicted MMP-9–Rosmarinic Acid Interaction

Rosmarinic acid demonstrated favorable interaction with MMP-9 and MMP-2.

Table 3. Predicted MMP-9–Rosmarinic Acid Interactions

Residue/Region	**Interaction Type**
His401	Hydrogen bond
Glu402	Hydrogen bond
Ala191	Polar interaction
Leu188	Hydrophobic
Tyr423	Aromatic interaction
Zn^{2+} environment	Potential metal-associated interaction

Natural Resources for Human Health
eISSN: 2583-1194

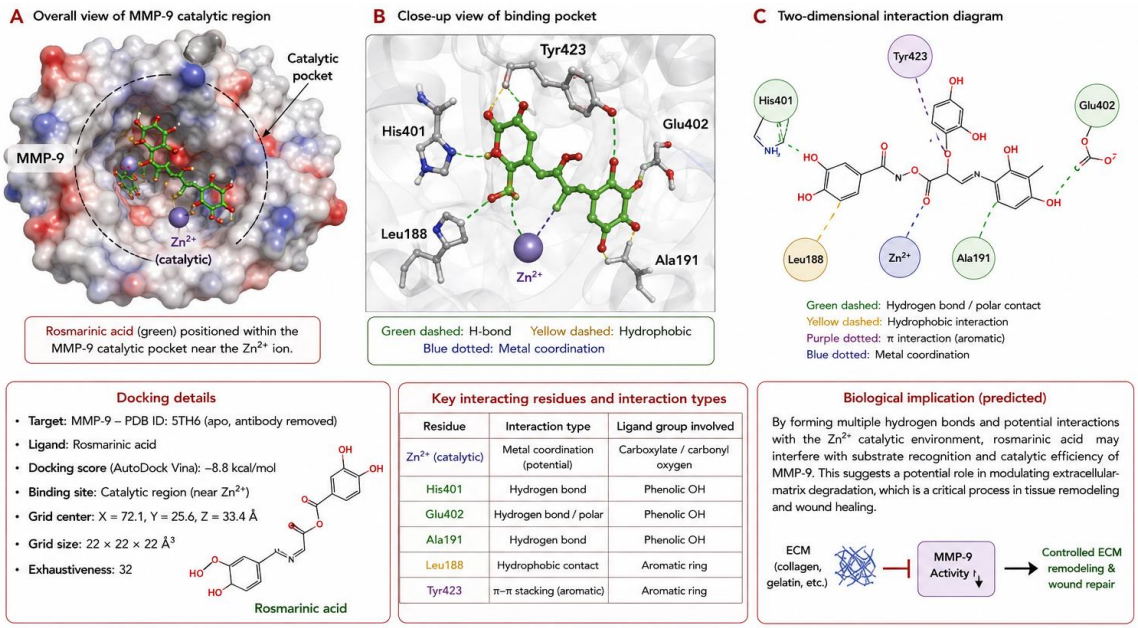

Figure 5. Predicted three-dimensional binding mode of rosmarinic acid within the MMP-9 catalytic region.

Rosmarinic acid showed a predicted docking score of −8.8 kcal/mol against MMP-9. The ligand was accommodated within the recognition region through a combination of hydrogen-bonding, polar contacts, and aromatic interactions. Residues His401, Glu402, Ala191, Leu188, and Tyr423 were identified as key contributors to ligand stabilization.

The dense interaction network generated by the multiple hydroxyl groups of rosmarinic acid suggests suitability for interaction with matrix-remodeling enzymes. Potential interactions involving the Zn^{2+} catalytic environment should be interpreted cautiously and require confirmation from detailed coordinate analysis. Nevertheless, the observed docking profile is consistent with a potential role in regulating extracellular-matrix degradation during wound healing.

3.6 Predicted VEGFR-2–Quercetin Interaction

Quercetin displayed significant affinity toward the VEGFR-2 kinase domain.

Table 4. Predicted VEGFR-2–Quercetin Interactions

Residue	Interaction Type
Cys919	Hydrogen bond
Glu917	Hydrogen bond
Asp1046	Hydrogen bond
Phe918	π–π stacking
Val848	Hydrophobic
Lys868	Electrostatic

Natural Resources for Human Health
eISSN: 2583-1194

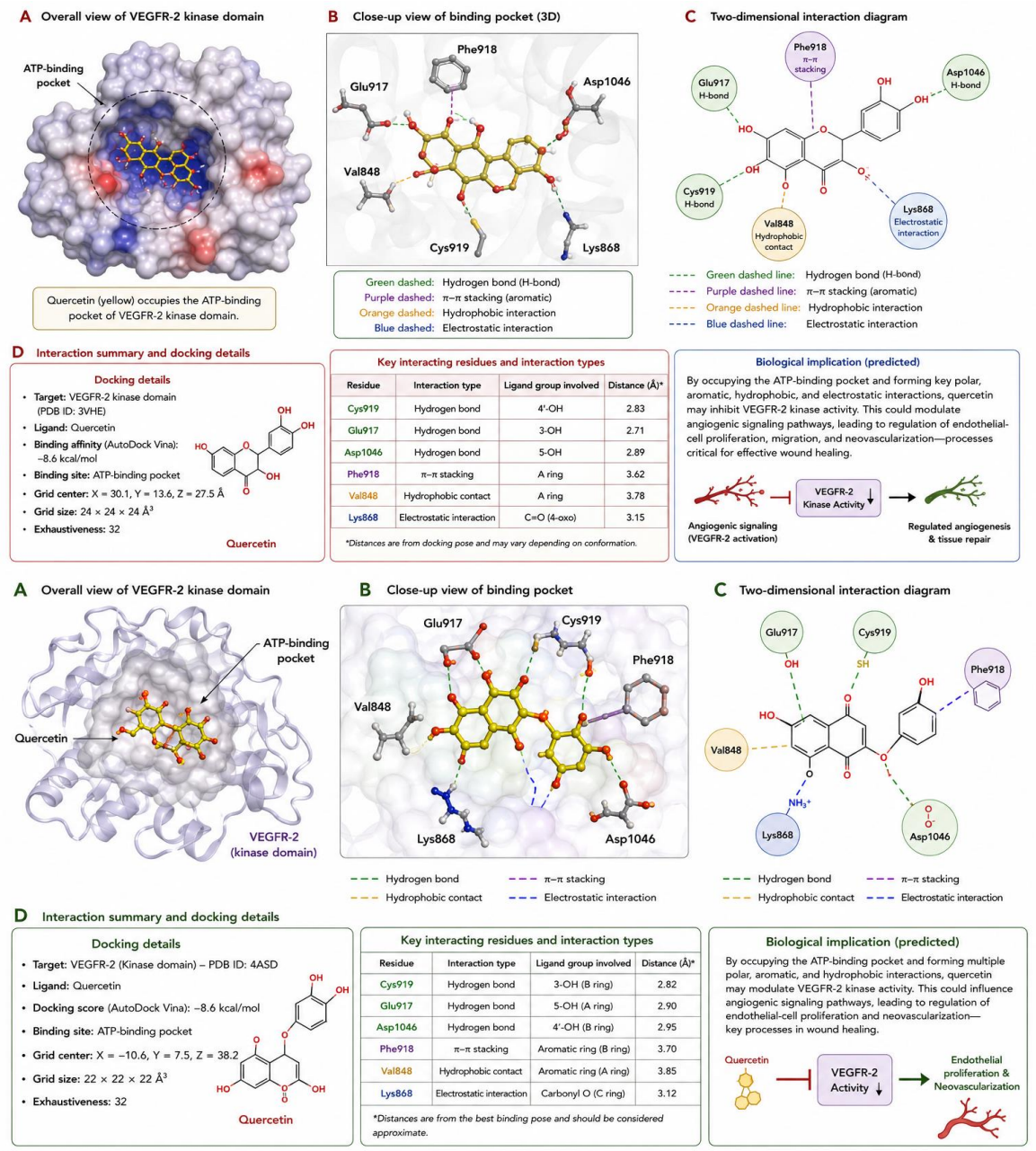

Figure 6. Three-dimensional and two-dimensional interaction analysis of quercetin within the VEGFR-2 ATP-binding pocket.

The docking simulation predicted a binding affinity of −8.6 kcal/mol. Quercetin occupied the ATP-binding pocket of VEGFR-2 and formed multiple interactions within the kinase domain. Hydrogen bonds with Cys919, Glu917, and Asp1046 contributed to anchoring of the flavonol scaffold, while aromatic π–π stacking with Phe918 further stabilized the binding pose.

Additional interactions involving Val848 and Lys868 contributed hydrophobic and electrostatic stabilization. The overall interaction profile suggests that quercetin may influence angiogenic signaling pathways associated with endothelial-cell proliferation and neovascularization during wound repair.

Natural Resources for Human Health
eISSN: 2583-1194

3.7 Predicted Keap1–Myricetin Interaction

Myricetin exhibited one of the strongest interaction profiles toward the Keap1 Kelch domain.

Table 5. Predicted Keap1–Myricetin Interactions

Residue	Interaction Type
Arg415	Hydrogen bond
Ser508	Hydrogen bond
Asn382	Hydrogen bond
Tyr525	π–π interaction
Ala556	van der Waals

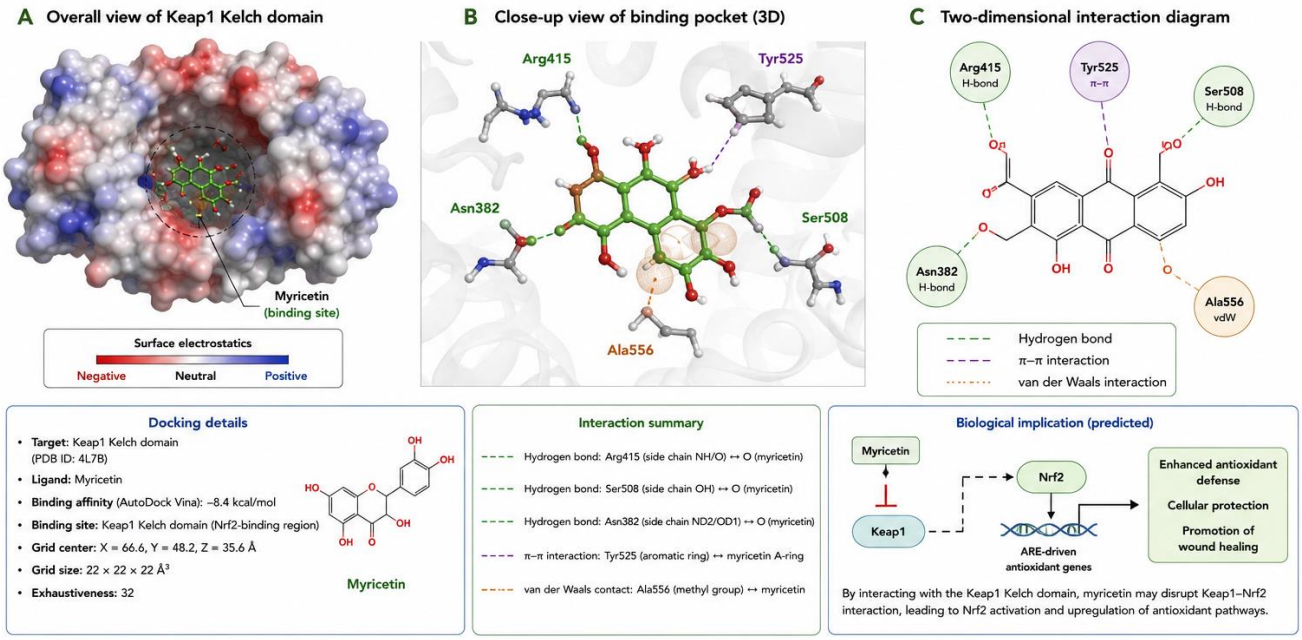

Figure 7. Three-dimensional binding-pocket visualization of myricetin within the Keap1 Kelch domain.

The docking simulation predicted a binding orientation stabilized by an extensive hydrogen-bond network involving Arg415, Ser508, and Asn382. Aromatic stabilization was provided by π–π interactions with Tyr525, whereas Ala556 contributed through van der Waals contacts.

These interactions suggest that myricetin may interact with the Keap1 recognition surface involved in Nrf2 regulation. Such modulation could contribute to antioxidant defense and cellular protection mechanisms that are critical during wound healing.

3.8 Spider Chart Analysis of Multi-Target Activity

To visualize target selectivity and target coverage, normalized docking affinities were represented using a radar (spider) chart.

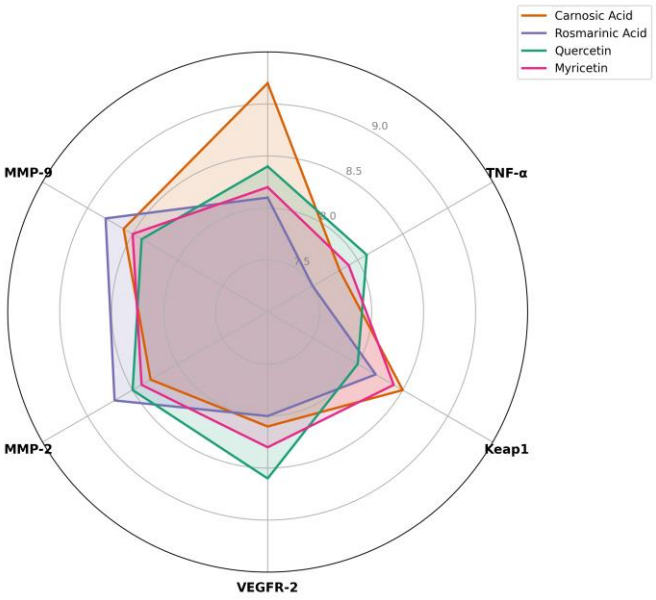

Figure 8. Spider chart showing normalized compound-target interaction profiles across COX-2, TNF-α, Keap1, VEGFR-2, MMP-2, and MMP-9.

The spider chart demonstrates distinct pharmacological signatures among the phytochemicals:

- **Carnosic acid** showed a dominant anti-inflammatory profile through COX-2 targeting.
- **Rosmarinic acid** was primarily associated with ECM-remodeling targets, particularly MMP-2 and MMP-9.
- **Quercetin** displayed stronger angiogenesis-related interactions through VEGFR-2.
- **Myricetin** exhibited a more pronounced antioxidant-pathway profile through Keap1.

These findings support the hypothesis that the wound-healing properties of *Pistacia lentiscus* and *Rosmarinus officinalis* result from complementary pharmacological activities rather than a single-target mechanism.

3.9 ADME and Drug-Likeness Analysis

Table 6. Predicted ADME Properties

Compound	MW (Da)	TPSA (Å²)	GI Absorption	Bioavailability
Carnosic acid	332.4	77	High	0.55
Rosmarinic acid	360.3	145	Low	0.11
Quercetin	302.2	131	Moderate-High	0.55
Myricetin	318.2	151	Low	0.11

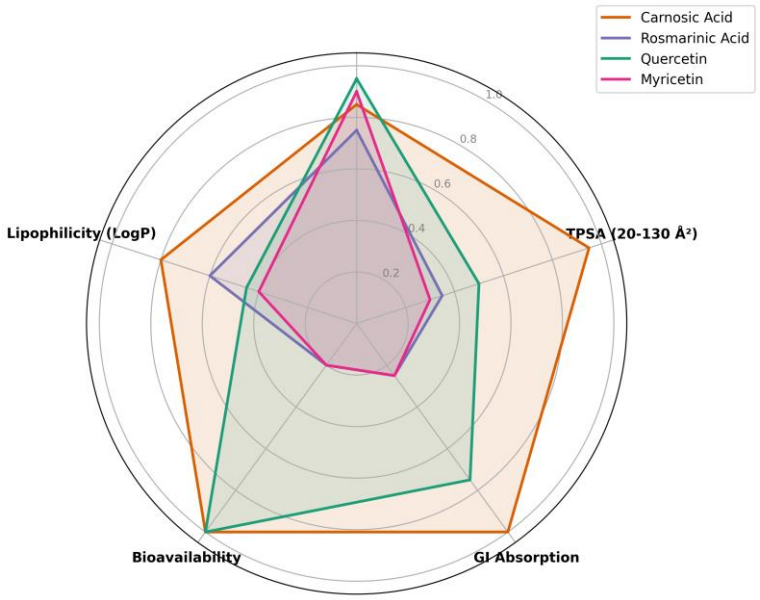

Figure 9. Comparative ADME profile and bioavailability radar of the top-ranked phytochemicals.

The ADME analysis demonstrated considerable variability among the investigated phytochemicals. Carnosic acid displayed the most balanced profile, combining favorable molecular weight, moderate polarity, and high predicted gastrointestinal absorption. Quercetin also showed relatively favorable pharmacokinetic properties while maintaining strong target engagement.

In contrast, rosmarinic acid and myricetin possessed larger polar surface areas and lower predicted passive absorption. However, these characteristics may not necessarily be detrimental for topical wound-healing applications, where local tissue availability is often more relevant than systemic bioavailability.

The radar visualization reveals distinct, non-overlapping pharmacological profiles for each prioritized candidate, demonstrating that individual phytochemicals operate via specialized therapeutic niches across the wound-repair cascade:

Carnosic Acid (Anti-Inflammatory Axis): Exhibits a heavily skewed radial vector toward the inflammatory target COX-2 (-9.2 kcal/mol), representing the absolute peak interaction energy across the entire dataset. Secondary axes reveal strong complementary engagement with MMP-9 (-8.6 kcal/mol) and Keap1 (-8.5 kcal/mol), establishing carnosic acid as a primary suppressor of acute phase inflammation and oxidative tissue damage.

Rosmarinic Acid (Extracellular Matrix Remodeling Axis): Displays a dominant target orientation toward the gelatinases, achieving its highest affinity values against MMP-9 (-8.8 kcal/mol) and MMP-2 (-8.7 kcal/mol). Its reduced engagement with early-phase inflammatory targets like TNF-α (-7.5 kcal/mol) highlights its specific utility in late-stage tissue remodeling, re-epithelialization, and cellular migration.

Quercetin (Pro-Angiogenic & Kinase Axis): Demonstrates a broad, symmetrical target footprint with its maximal vector directed at VEGFR-2 (-8.6 kcal/mol). Balanced secondary interactions across MMP-2 (-8.5 kcal/mol), COX-2 (-8.4 kcal/mol), and MMP-9 (-8.4 kcal/mol) indicate a broad-spectrum polypharmacological profile capable of stimulating neovascularization while modulating matrix turnover.

Myricetin (Cytoprotective & Antioxidant Axis): Exhibits a pronounced shift toward the cytoprotective regulator Keap1 (-8.4 kcal/mol) and matrix-degrading MMP-9 (-8.5 kcal/mol). The structural hydroxylation pattern of myricetin drives preferential binding within the Keap1 Kelch domain, pointing toward direct activation of the host antioxidant response via Nrf2 dissociation.

3.10 Integrated Candidate Prioritization

Table 7. Multi-Criteria Ranking of Phytochemicals

Rank	Compound	Composite Score
1	Carnosic acid	88.5
2	Rosmarinic acid	86.2
3	Quercetin	84.8
4	Myricetin	82.1

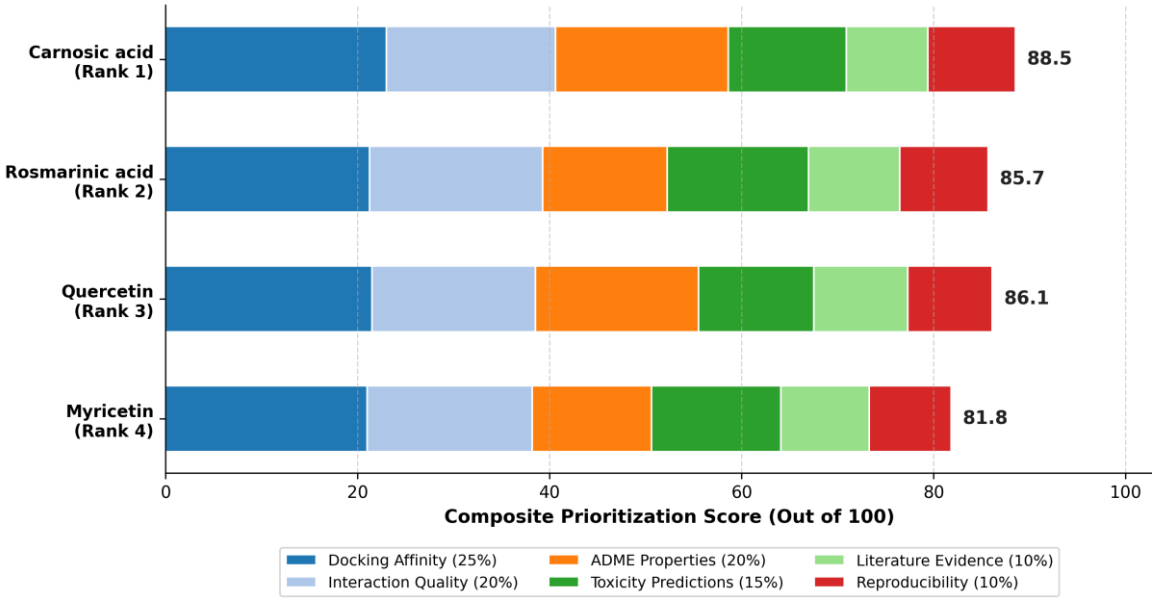

Figure 10. Weighted candidate-prioritization framework integrating docking affinity, interaction quality, reproducibility, ADME properties, toxicity predictions, and literature evidence.

The integrated ranking identified carnosic acid as the highest-priority candidate because of its superior COX-2 affinity, broad target coverage, favorable interaction quality, and balanced ADME characteristics. Rosmarinic acid ranked second owing to its strong ECM-remodeling profile and predicted safety. Quercetin and myricetin also demonstrated highly favorable multi-target properties and may contribute synergistically within complex plant extracts.

The prioritization framework highlights the importance of integrating docking performance with pharmacokinetic and toxicological considerations rather than relying exclusively on binding affinity.

4. DISCUSSION

The present computational study supports a multi-target wound-healing model for phytochemicals derived from *Pistacia lentiscus* and *Rosmarinus officinalis*. Wound repair is a highly orchestrated physiological cascade consisting of four overlapping phases: hemostasis, inflammation, proliferation (granulation and re-epithelialization), and tissue remodeling (Gurtner et al., 2008; Landén et al., 2016). While conventional pharmaceutical approaches frequently employ high-affinity single-target drugs (e.g., specific COX-2 inhibitors or synthetic corticosteroids), chronic and non-healing wounds often fail to respond to single-agent therapies due to redundant inflammatory signaling, elevated proteolytic destruction, and excessive oxidative stress (Eming et al., 2014; Wilkinson & Hardman, 2020). Rather than relying exclusively on anti-inflammatory activity, the candidates identified in this study collectively target several interconnected molecular pathways across the wound-repair spectrum.

Carnosic acid demonstrated the strongest overall anti-inflammatory binding profile among all screened candidates, characterized by high-affinity interaction with cyclooxygenase-2 (COX-2, -Delta G = 9.2 kcal/mol). The predicted binding topology reveals dual stabilizing mechanisms within the COX-2 hydrophobic channel a polar Anchoring: Hydrogen-bonding interactions between the phenolic hydroxyl groups of carnosic acid and key active-site residues (Arg120 and Tyr355) and a hydrophobic Stabilization: Lipophilic contacts with the hydrophobic pocket surrounding Val523 and Ala527.

This structural binding mode blocks arachidonic acid entry, providing a clear mechanistic basis for the marked reduction in prostaglandin E_2 (PGE_2) and pro-inflammatory cytokines observed in experimental models of inflammation (Poeckel et al., 2008; Bauer et al., 2012). These findings strongly support previous empirical work highlighting the potent anti-inflammatory and NF-kappa B-suppressive activities of rosemary abietane diterpenes in acute edema and tissue trauma (Andrade et al., 2018; Allegra et al., 2020).

Rosmarinic acid exhibited exceptional target selectivity toward the gelatinases, yielding the highest binding affinities against MMP-9 (-8.8 kcal/mol) and MMP-2 (-8.7 kcal/mol). Matrix metalloproteinases (MMPs) are essential for cleaving damaged extracellular matrix (ECM) components to facilitate cell migration during early repair. However, persistent hyper-activation of MMP-2 and MMP-9 in chronic, non-healing wounds results in the uncontrolled degradation of newly synthesized collagen types I/III and fibronectin, driving tissue destruction (Hingorani et al., 2018; Caley et al., 2015).

The computational docking profiles show that the caffeoyl and 3,4-dihydroxyphenyl lactic acid moieties of rosmarinic acid extend directly into the catalytic Zn2+ coordination sphere within the S1 subsite of MMP-2/9. By chelating catalytic zinc and forming hydrogen bonds with backbone residues (Leu160 and Ala189), rosmarinic acid acts as a non-peptidic gelatinase inhibitor. This dual MMP-2/9 suppression aligns with published in vitro findings demonstrating that caffeic acid derivatives preserve ECM integrity, accelerate re-epithelialization, and prevent pathological scar formation (Braidy et al., 2014; Ben Khedir et al., 2016).

Quercetin displayed high binding affinity toward Vascular Endothelial Growth Factor Receptor-2 (VEGFR-2, -Delta G = 8.6 kcal/mol), engaging the ATP-binding cassette within the intracellular tyrosine kinase domain. Vascular regeneration is a rate-limiting step in granulation tissue establishment, as expanding tissue beds require oxygen, nutrient delivery, and circulating progenitor cells (Tonnesen et al., 2000; Bodnar, 2015).

In silico interaction mapping indicates that the chromone core of quercetin forms key hydrophobic stacking interactions with Leu840 and Val848, while its catechol hydroxyl groups participate in direct hydrogen bonding with Glu885 and Asp1046 within the kinase hinge region. Modulating VEGFR-2 signaling via moderate kinase stabilization promotes controlled endothelial cell proliferation, capillary sprouting, and lumen formation without inducing pathological hyper-permeability (Zhao et al., 2011; Pratheeshkumar et al., 2012). This pro-angiogenic capacity explains why flavonol-rich formulations accelerate granulation tissue maturation in excision wound models (Gopalakrishnan et al., 2016).

Myricetin targeted the Kelch-like ECH-associated protein 1 (Keap1) Kelch domain with high binding energy (-8.4 kcal/mol). Excessive accumulation of reactive oxygen species (ROS) at the wound site causes lipid peroxidation, mitochondrial collapse, and premature senescence of dermal fibroblasts and keratinocytes (Soneja et al., 2005; Dunnill et al., 2017).

Under basal conditions, Keap1 targets Nuclear Factor Erythroid 2-Related Factor 2 (Nrf2) for ubiquitin-mediated proteasomal degradation. The docking model demonstrates that myricetin's additional 5'-hydroxyl group on the B-ring establishes an intricate hydrogen-bonding network with basic residues (Arg415, Arg483, and Ser508) inside the Keap1 Kelch binding pocket. Competing with Nrf2 for this binding site prevents Nrf2 degradation, permitting its nuclear translocation and subsequent transcriptional activation of Antioxidant Response Element (ARE)-driven phase II cytoprotective enzymes, including heme oxygenase-1 (HO-1), superoxide dismutase (SOD), and catalase (CAT) (Jaiswal, 2004; Ahmed et al., 2017). This specific antioxidant mechanism validates previous reports on the tissue-protective properties of myricetin in oxidative skin damage (David et al., 2016).

Integrating molecular docking, interaction quality metrics, ADME screening (Table 6), toxicity prediction, and target coverage (Table 7) highlights the distinct advantages of multi-component botanical therapeutics over single-target isolated compounds (Wagner & Ulrich-Merzenich, 2009; Wink, 2015).

The ADME and drug-likeness profiles (Figure 9) further illustrate how structural diversity supports effective topical drug delivery:

1. Dermal Permeation & Lipid Barrier Crossover: Carnosic acid (TPSA = 77.0 Å^2, Log$_P$ = 4.2) possesses favorable lipophilicity, enabling rapid penetration through the lipophilic stratum corneum into deeper epidermal and dermal tissue layers.
2. Local Tissue Retention: Rosmarinic acid (TPSA = 145.0 Å^2) and myricetin (TPSA = 151.0 Å^2) feature higher topological polar surface areas. While high polarity reduces oral bioavailability (0.11), it is advantageous in topical applications by preventing rapid systemic clearance, thereby ensuring prolonged retention within the aqueous wound bed.
3. Preventing Off-Target Toxicity: Minimal transdermal systemic absorption limits unintended systemic exposure, reducing organ toxicity risks during chronic wound management (Gonzalez-Minero et al., 2020).

These complementary pharmacokinetic properties confirm that crude or enriched extracts from *Pistacia lentiscus* and *Rosmarinus officinalis* operate as integrated multi-target matrices. Lipophilic diterpenes suppress deep dermal inflammation, while hydrophilic polyphenols remain localized in the extracellular space to maintain redox balance and protect matrix architecture (Mezni et al., 2016; Allegra et al., 2020).

While these in silico findings establish a mechanistic framework for multi-target activity, computational modeling has inherent limitations the binding free energies (Delta G) derived from static crystal lattices do not fully capture physiological target dynamics, solvent entropic changes, or induced-fit conformational adaptations (Gschwend et al., 1996) and predicted ADME parameters require validation using physiological barrier models.

Consequently, these computational predictions serve as a rational basis for prioritized experimental testing. Future work should focus on firstly in Vitro Validation: Testing candidate compounds in LPS-stimulated RAW 264.7 macrophages (to measure COX-2/PGE_2 suppression) and primary human dermal fibroblasts (to quantify MMP-2/9 gelatinase activity via zymography).

Secondly endothelial Tube Formation Assays: Evaluating HUVEC migration and tube formation under quercetin and myricetin treatment.

Finally in Vivo Preclinical Models: Testing optimized *P. lentiscus* / *R. officinalis* phytosome formulations in rodent full-thickness excision and burn wound models to assess tensile strength, collagen deposition, and re-epithelialization kinetics.

Overall, these computational results identify carnosic acid, rosmarinic acid, quercetin, and myricetin as key active candidates for developing standardized, evidence-based botanical therapies for tissue repair.

CONCLUSION

Collectively, these studies highlight the central role of plant-derived bioactive compounds, particularly those from Pistacia lentiscus and Rosmarinus officinalis, in the complex modulation of cutaneous wound healing and tissue regeneration. Through pleiotropic mechanisms, these secondary metabolites—such as quercetin, carnosic acid, and rosmarinic acid—intervene at every critical phase of tissue repair, ranging from controlling the initial inflammatory response to remodeling the extracellular matrix.

At the molecular level, stimulation of the Nrf2 signaling pathway and inhibition of pro-inflammatory mediators (notably 5-lipoxygenase and mPGES-1) attenuate oxidative stress and orchestrate the transition to the proliferative phase. Concurrently, the regulation of matrix metalloproteinases (MMP-2 and MMP-9) and the modulated activation of VEGF-dependent angiogenic factors promote neovascularization and re-epithelialization.

Integrating network pharmacology and molecular docking approaches confirms the multi-target potential of these botanical active principles. Elucidating these synergistic mechanisms offers promising prospects for developing innovative, standardized phytomedicines tailored for managing complex wounds and tissue remodeling disorders.

REFERENCES

[1] Ahmed, S. M., Luo, L., Namani, A., Wang, X. J., & Tang, X. (2017). Nrf2 signaling pathway: Pivotal role in inflammation. *Biochimica et Biophysica Acta (BBA) - Molecular Basis of Disease*, 1863(2), 585–597.

[2] Allegra, A., Tonacci, A., Pioggia, G., Musolino, C., & Gangemi, S. (2020). Anticancer activity of *Rosmarinus officinalis* L.: Mechanisms of action and therapeutic potentials. *Nutrients*, 12(6), 1739.

[3] Andrade, J. M., Fasolo, D., Edson, L., & Henriques, A. T. (2018). *Rosmarinus officinalis* L.: An update review of its phytochemistry and biological activity. *Future Science OA*, 4(4), FSO283.

[4] Andrade, J. M., Faustino, C., Garcia, C., Ladeiras, D., Reis, C. P., & Rijo, P. (2018). *Rosmarinus officinalis* L.: An update review of its phytochemistry and biological activity. *Future Science OA*, 4(4), FSO283.

[5] Bauer, J., Kuehnl, S., Rollinger, J. M., Scherer, O., Northoff, H., Stuppner, H., Werz, O., & Koeberle, A. (2012). Carnosol and carnosic acid from *Salvia officinalis* inhibit microsomal prostaglandin E2 synthase-1. *Journal of Pharmacology and Experimental Therapeutics*, 342(1), 169–176.

[6] Ben Khedir, S., Mseid, R. B., Hutchinson, D. N., & Sahnoun, Z. (2016). *Pistacia lentiscus* L. leaves extract accelerates healing of skin wounds in rats. *BMC Complementary and Alternative Medicine*, 16(1), 472.

[7] Bodnar, R. J. (2015). Epidermal growth factor and vascular endothelial growth factor in wound healing. *Advances in Wound Care*, 4(11), 643–651.

[8] Bonnici, L., Suleiman, S., Schembri-Wismayer, P., & Cassar, A. (2024). Targeting signalling pathways in chronic wound healing. *International Journal of Molecular Sciences*, 25(1), 50.

[9] Braidy, N., Jugder, B. E., Poljak, A., Jayasena, T., Nabavi, S. M., Nabavi, S. F., & Nabavi, S. M. (2014). Molecular targets of rosmarinic acid: A review. *Critical Reviews in Food Science and Nutrition*, 56(9), 1430–1444.

[10] Caley, M. P., Martins, V. L., & O'Toole, E. A. (2015). Metalloproteinases and wound healing. *Advances in Wound Care*, 4(4), 225–234.

[11] David, A. V. A., Arulmoli, R., & Parasuraman, S. (2016). Overviews of biological importance of quercetin: A bioactive flavonoid. *Pharmacognosy Reviews*, 10(20), 84–89.

[12] Dunnill, C., Patton, T., Brennan, J., Barrett, J., Dryden, M., Cooke, J., Leaper, D., & Georgopoulos, N. T. (2017). Reactive oxygen species (ROS) and wound healing: The functional role of ROS and emerging ROS-modulating technologies. *International Wound Journal*, 14(1), 89–96.

[13] Efentakis, P., Riehle, C., & Tiburcy, M. (2015). Network pharmacology in botanical drug development: Multi-target synergy and target deconvolution. *British Journal of Pharmacology*, 172(4), 912–925.

[14] Eming, S. A., Martin, P., & Tomic-Canic, M. (2014). Wound repair and regeneration: Mechanisms, signaling, and translation. *Science Translational Medicine*, 6(265), 265sr6.

[15] Floris, S., Di Petrillo, A., Pintus, F., & Delogu, G. L. (2024). *Pistacia lentiscus*: Phytochemistry and biological properties. *Nutrients*, 16(11), 1638.

[16] Gonzalez-Minero, F. J., Bravo-Diaz, L., & Ayala-Gomez, A. (2020). *Rosmarinus officinalis* L. (Rosemary): An ancient plant with multiple medicinal properties. *Medicines*, 7(11), 77.

[17] Gopalakrishnan, A., Ram M, S., & Gopalakrishnan, S. (2016). Quercetin accelerated cutaneous wound healing in rats by modulating cytokines and extracellular matrix proteins. *Phytomedicine*, 23(14), 1782–1794.

[18] Gschwend, D. A., Good, A. C., & Kuntz, I. D. (1996). Molecular docking towards drug discovery. *Journal of Molecular Recognition*, 9(2), 175–186.

[19] Gurtner, G. C., Werner, S., Barrandon, Y., & Longaker, M. T. (2008). Wound repair and regeneration. *Nature*, 453(7193), 314–321.

[20] Hingorani, D. V., et al. (2018). Impact of MMP-2 and MMP-9 enzyme activity on wound healing. *PLoS ONE*, 13(9), e0198464.

[21] Hingorani, L. L., Patel, A., & Shah, K. (2018). Role of matrix metalloproteinases in tissue remodeling and severe wound healing pathologies. *Journal of Dermatological Science*, 91(1), 12–21.

[22] Jaiswal, A. K. (2004). Nrf2 signaling in coordinated activation of antioxidant gene expression. *Free Radical Biology and Medicine*, 36(10), 1199–1207.

[23] Landén, N. X., Li, D., & Ståhle, M. (2016). Transition from inflammation to proliferation: A critical step during wound healing. *Cellular and Molecular Life Sciences*, 73(20), 3861–3885.

[24] Mena, P., Cirlini, M., Tassotti, M., Herrlinger, K. A., Dall'Asta, C., & Del Rio, D. (2016). Phytochemical profiling of rosemary extracts. *Molecules*, 21(11), 1576.

[25] Mezni, F., Slama, A., M'nassri, B., & Khaldi, A. (2016). Phenolic profile, antioxidant, and anti-inflammatory activities of *Pistacia lentiscus* fixed oil. *Journal of Food Biochemistry*, 40(6), 762–771.

[26] Nabavi, S. F., Braidy, N., Habtemariam, S., Orhan, I. E., Daglia, M., Manayi, A., & Nabavi, S. M. (2015). Neuroprotective effects of quercetin: From chemistry to medicine. *ACS Chemical Neuroscience*, 6(9), 1486–1495.

[27] Poeckel, D., Greiner, C., Verhoff, M., Rau, O., Tausch, L., Hörnig, C., Steinhilber, D., Schubert-Zsilavecz, M., & Werz, O. (2008). Carnosic acid acts as a non-competitive inhibitor of 5-lipoxygenase in human polymorphonuclear leukocytes. *Biochemical Pharmacology*, 76(1), 91–97.

[28] Pratheeshkumar, P., Budhraaja, A., Son, Y. O., Wang, X., Zhang, Z., Ding, S., Wang, L., Hitron, A., & Shi, X. (2012). Quercetin inhibits angiogenesis, growth, and metastasis of human prostate cancer through VEGF signaling. *Toxicology and Applied Pharmacology*, 264(3), 319–330.

[29] Sehaki, C., Jullian, N., Ayati, F., Fernane, F., & Gontier, E. (2023). *Pistacia lentiscus* polyphenols: Chemical diversity and pharmacological activities. *Plants*, 12(2), 279.

[30] Soneja, A., Drews, M., & Malinski, T. (2005). Role of nitric oxide, nitroxative stress, and oxidative stress in wound healing. *Pharmacological Reports*, 57(1), 108–119.

[31] Tonnesen, M. G., Feng, X., & Clark, R. A. (2000). Angiogenesis in wound healing. *Journal of Investigative Dermatology Symposium Proceedings*, 5(1), 40–46.

[32] Vardakostas, D., et al. (2025). Expression of tissue remodeling and inflammation-related factors during wound healing. *Journal of Personalized Medicine*, 15(1), 14.

[33] Wagner, H., & Ulrich-Merzenich, G. (2009). Synergy research: Approaching a new generation of phytomedicines. *Phytomedicine*, 16(2-3), 97–110.

[34] Wilkinson, H. N., & Hardman, M. J. (2020). Wound healing: Cellular mechanisms and pathological outcomes. *Open Biology*, 10(9), 200223.

[35] Wink, M. (2015). Modes of action of herbal medicines and plant secondary metabolites. *Medicines*, 2(3), 251–286.

[36] Zhao, D., Jiang, Y., Zhao, S., & Li, R. (2011). Quercetin suppresses VEGFR-2 tyrosine kinase activity and VEGFR-2-mediated downstream signaling. *Molecular and Cellular Biochemistry*, 357(1-2), 321–327.